Kif26b, a kinesin family gene, regulates adhesion of the embryonic kidney mesenchyme

Yukako Uchiyama[a,b,1], Masaji Sakaguchi[a,b,c,1], Takeshi Terabayashi[a,b], Toshiaki Inenaga[a], Shuji Inoue[a,b], Chiyoko Kobayashi[a], Naoko Oshima[d], Hiroshi Kiyonari[d], Naomi Nakagata[e], Yuya Sato[f], Kiyotoshi Sekiguchi[f], Hiroaki Miki[g], Eiichi Araki[c], Sayoko Fujimura[a], Satomi S. Tanaka[a], and Ryuichi Nishinakamura[a,b,2]

[a]Department of Kidney Development, Institute of Molecular Embryology and Genetics, Kumamoto University, Kumamoto 860-0811, Japan; [b]Global COE "Cell Fate Regulation Research and Education Unit," Kumamoto University, Kumamoto 860-0811, Japan; [c]Department of Metabolic Medicine, Graduate School of Medical Sciences, Kumamoto University, Kumamoto 860-8556, Japan; [d]Laboratory for Animal Resources and Genetic Engineering, RIKEN Center for Developmental Biology, Kobe 650-0047, Japan; [e]Division of Reproductive Engineering, Center for Animal Resources and Development, Kumamoto University, Kumamoto 860-0811, Japan; [f]Laboratory of Extracellular Matrix Biochemistry, Institute for Protein Research, Osaka University, Osaka 565-0871, Japan; and [g]Laboratory of Intracellular Signaling, Institute for Protein Research, Osaka University, Osaka 565-0871, Japan

Edited by Eric N. Olson, University of Texas Southwestern, Dallas, TX, and approved April 15, 2010 (received for review November 27, 2009)

The kidney develops through reciprocal interactions between two precursor tissues: the metanephric mesenchyme and the ureteric bud. We previously demonstrated that the zinc finger protein Sall1 is essential for ureteric bud attraction toward the mesenchyme. Here, we show that *Kif26b*, a kinesin family gene, is a downstream target of *Sall1* and that disruption of this gene causes kidney agenesis because of impaired ureteric bud attraction. In the *Kif26b*-null metanephros, compact adhesion between mesenchymal cells adjacent to the ureteric buds and the polarized distribution of integrin α8 were impaired, resulting in failed maintenance of *Gdnf*, a critical ureteric bud attractant. Overexpression of Kif26b in vitro caused increased cell adhesion through interactions with nonmuscle myosin. Thus, Kif26b is essential for kidney development because it regulates the adhesion of mesenchymal cells in contact with ureteric buds.

kinesin | Gdnf | kidney development | metanephric mesenchyme | Sall1

In the developing kidney, the metanephric mesenchyme secretes glial cell line-derived neurotrophic factor (GDNF), which induces the budding of ureteric buds from the Wolffian duct. Upon contact with ureteric buds, adjacent metanephric mesenchymal cells condense around the tips of the ureteric buds. Concomitantly, integrin α8 expressed in the mesenchyme is polarized on the cell surface facing the ureteric buds. Integrin α8 interacts with its ligand nephronectin expressed on the surface of the ureteric bud epithelia. This interaction is essential for the maintenance, but not the initiation, of *Gdnf* expression in the mesenchyme and for further attraction of ureteric buds, although the precise mechanisms remain unknown. Thus, genetic ablation of nephronectin or integrin α8 results in the failure of *Gdnf* maintenance and kidney agenesis (1, 2). Subsequently, Wnt9b secreted from the ureteric buds induces Wnt4 expression in the mesenchyme (3). Wnt4 functions in a cell-autonomous manner to transform the mesenchyme to epithelia, which differentiate into each segment of nephrons, including the glomerulus, proximal tubule, Henle's loop, and distal tubule (4). This Wnt4-mediated differentiation is antagonized by the transcription factor Six2 that functions to maintain nephron progenitors (5, 6).

We previously reported that the nuclear zinc-finger protein Sall1 is essential for ureteric bud attraction in kidney development and that metanephric mesenchymal cells that highly express Sall1 contain multipotent nephron progenitors (7, 8). To examine the molecular pathways regulated by Sall1, we searched for genes that are predominantly expressed in Sall1-positive mesenchymal cells by cDNA microarray analysis using *Sall1-GFP* knock-in mice (9). Here, we describe that *Kif26b*, a kinesin family gene, acts downstream of *Sall1* and regulates the adhesion of mesenchymal cells surrounding ureteric buds, providing insights into the mechanisms of kidney development.

Results

Kif26b Is Expressed in the Metanephric Mesenchyme During Nephrogenesis. Mouse full-length *Kif26b* encodes a 2,112-aa protein that shows 87% amino acid homology with human *KIF26B* and has a well conserved motor domain (96% identical to human *KIF26B*) in the N terminus (GenBank accession no. AB355846). Kinesins constitute a large family of intracellular motor proteins, some of which transport cargos along microtubules. Forty-five members have so far been identified in mice and humans, and are involved in many processes such as organelle transport, intraflagellar transport, and cell signaling (10). The functions of *Kif26b*, which is classified into the kinesin-11 family, remain unknown (11).

We first examined *Kif26b* expression in the embryonic kidney by in situ hybridization. *Kif26b* was detected in the metanephric mesenchyme at embryonic day (E) 10.5 (Fig. 1*A*). After E11.5, its expression was observed in mesenchymal cells surrounding the tips of ureteric buds in the metanephroi (Fig. 1 *B* and *C*). At E14.5, *Kif26b* was strongly expressed in the nephrogenic zone (Fig. 1*D*, arrowheads) where the nephron progenitor marker *Six2* was also detected (Fig. 1*E*). Notably, among the *Sall1*-positive domains, *Kif26b* signals were only present in the uncommitted mesenchyme and absent from more differentiated structures including renal vesicles and comma-shaped bodies (Fig. 1*F*, arrow). Immunostaining showed that Kif26b protein was localized in the cytosol of mesenchymal cells (Fig. 1*G*). Furthermore, the expression of Kif26b was markedly reduced in *Sall1*-null metanephroi, suggesting that *Kif26b* is a genetic downstream target of *Sall1* in the metanephric mesenchyme (Fig. 1 *H* and *I*, and Fig. S1*A*). Indeed, multiple Sall1-binding consensus sequences were found in the *Kif26b* promoter (12), and a biotinylated oligonucleotide probe of this region, but not a mutated one, precipitated endogenous Sall1 protein in newborn kidney lysates (Fig. 1*J* and Fig. S1*B*). Chromatin immunoprecipitation (ChIP) using an anti-Sall1 antibody also confirmed Sall1 binding to the *Kif26b* promoter (Fig. 1*K*). Furthermore, overexpression of Sall1 enhanced

Author contributions: Y.U., M.S., and R.N. designed research; Y.U., M.S., T.T., T.I., S.I., C.K., S.F., and R.N. performed research; N.O., H.K., N.N., Y.S., and K.S. contributed new reagents/analytic tools; Y.U., M.S., T.T., T.I., K.S., H.M., E.A., S.S.T., and R.N. analyzed data; and Y.U. and R.N. wrote the paper.

The authors declare no conflict of interest.

This article is a PNAS Direct Submission.

Data deposition: The sequence reported in this paper has been deposited in the DNA Data Bank of Japan/European Molecular Biology Laboratory/GenBank databases (accession no. AB355846).

[1]Y.U. and M.S. contributed equally to this work.

[2]To whom correspondence should be addressed. E-mail: ryuichi@gpo.kumamoto-u.ac.jp.

This article contains supporting information online at www.pnas.org/lookup/suppl/doi:10.1073/pnas.0913748107/-/DCSupplemental.

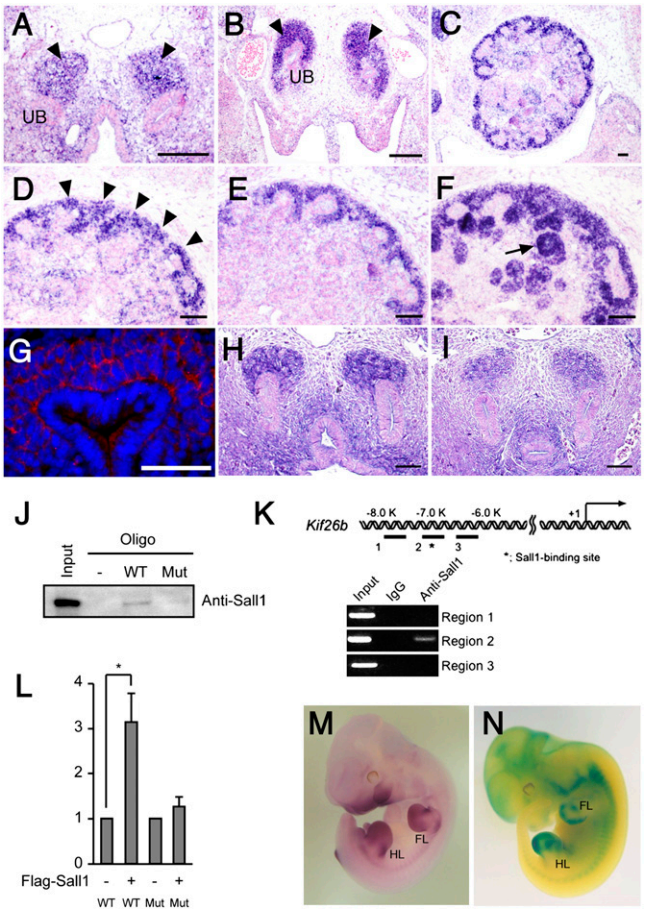

Fig. 1. Expression of Kif26b in the metanephric mesenchyme. (*A–F*) Transverse sections through the metanephric regions of mouse embryos at E10.5 (*A*), E11.5 (*B*), and E14.5 (*C–F*) stained by in situ hybridization for *Kif26b* (*A–D*), *Six2* (*E*), and *Sall1* (*F*). Arrowheads, mesenchymal cells; arrow, comma-shaped body; UB, ureteric bud. (Scale bars, 100 μm.) (*G*) Cytosolic localization of endogenous Kif26b protein. Sections of embryonic kidneys at E11.5 were immunostained with an anti-Kif26b antibody (red). Nuclei were visualized by DAPI staining. (Scale bar, 100 μm.) (*H* and *I*) Reduced Kif26b expression in the *Sall1*-null mesenchyme (*I*) at E11.5 compared with the wild-type mesenchyme (*H*), as evaluated by immunostaining for Kif26b. (Scale bars, 100 μm.) (*J*) Binding of endogenous Sall1 protein to the promoter sequences of *Kif26b*. Newborn kidney lysates were incubated with a biotinylated oligonucleotide probe, pulled down with streptavidin beads, and immunoblotted with an anti-Sall1 antibody. (*K*) ChIP analysis using embryonic kidney lysates and the anti-Sall1 antibody. The pulled down DNA was amplified for the *Kif26b* promoter sequences. (*L*) Activation of the *Kif26b* promoter activity by Sall1. (M) *Kif26b* expression in the limb buds and central nervous system, as evaluated by whole-mount in situ hybridization of *Kif26b* at E11.5. FL, forelimb; HL, hindlimb. (*N*) Whole-mount X-gal staining of a *Kif26b-lacZ* mouse at E11.5.

the activity of a luciferase construct fused to the *Kif26b* promoter (Fig. 1*L*). Thus, *Kif26b* is expressed in the metanephric mesenchyme and is a direct downstream target of *Sall1*. *Kif26b* was also detected in other parts of the embryos such as the limb buds and central nervous system (Fig. 1 *M* and *N*).

Kif26b Ablation Causes Kidney Agenesis Owing to Impaired Ureteric Bud Invasion into the Metanephric Mesenchyme. To examine whether *Kif26b* has a functional role in kidney development, we used gene targeting to generate *Kif26b*-deficient mice (Fig. S2). Heterozygous mice were viable and fertile, and offspring were born at the expected Mendelian frequency. However, *Kif26b*$^{-/-}$ mice died within 24 h after birth. At birth, 22 of 33 (66.7%) mutant mice showed bilateral kidney agenesis, 9 (27.3%) showed unilateral kidney agenesis and hypoplasia on the other side, and 2 (6.0%) had bilateral small kidneys (Fig. 2*A*). The remaining kidneys were significantly reduced in size, and the mesenchyme in the cortical nephrogenic zone had almost disappeared (Fig. 2*B*). The development of other organs was apparently normal. Although *Kif26b*-null kidneys showed no histological differences from wild-type kidneys until E10.5 (Fig. 2 *C* and *D*), ureteric bud attraction was impaired after E11.0 (Fig. 2 *E* and *F*). In the mutant embryos, the ureteric buds were attracted close to the mesenchyme but failed to invade and branch into the mesenchyme (Fig. 2 *G* to *J*), and the kidney disappeared by E14.5 (Fig. 2 *K* and *L*). The mesenchymal cells underwent apoptotic cell death at E12.5, as shown by cleaved caspase-3 staining (Fig. 2 *M* and *N*). Bilateral ureteric attraction failure was observed in 7 of 11 (63.6%) mutant embryos at E11.0–11.5, while the remaining mutant embryos showed invasion of the ureteric bud on one side (2 of 11, 18.2%) or both sides (2 of 11, 18.2%), although to lesser extents compared with the wild-type embryos. These frequencies were fairly well correlated with those of the renal abnormalities in the newborn mice. Therefore, *Kif26b* is essential for ureteric bud attraction and could be one of the major functional molecules

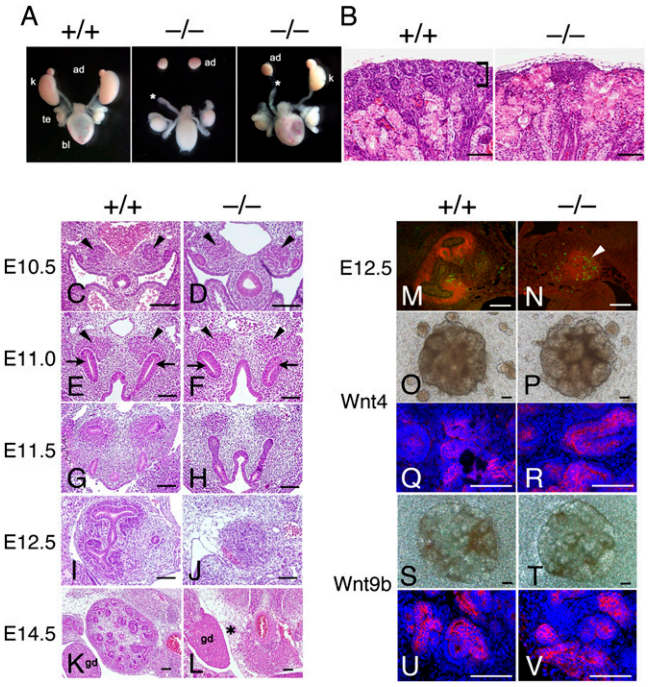

Fig. 2. Kidney agenesis and impaired ureteric bud attraction in *Kif26b*-null mutants. (*A*) Urogenital tissues from wild-type (*Left*) and *Kif26b*-null (*Center* and *Right*) newborn mice. ad, adrenal gland; k, kidney; te, testis; bl, bladder. Asterisk, blind-ended ureter. (*B*) Hematoxylin and eosin staining of a wild-type kidney and a mutant remnant kidney in newborn mice. Square bracket, mesenchyme in the cortical nephrogenic zone. (Scale bars, 100 μm.) (*C–L*) Failure of ureteric bud attraction under *Kif26b* deficiency. Wild-type and *Kif26b*-null embryonic kidneys were stained with hematoxylin and eosin. Arrowheads, metanephric mesenchyme; arrows, ureteric buds; gd, gonad; asterisk, remnant kidney. (*M* and *N*) Cleaved caspase-3-positive cells (arrowhead) in the Sall1-positive mesenchyme in *Kif26b*-null embryos at E12.5. Sections were immunostained for Sall1 (red) and cleaved caspase-3 (green). (Scale bars, 100 μm.) (*O–R*) Intact potency for epithelial conversion of the *Kif26b*-null mesenchyme. Metanephric mesenchyme was cultured on 3T3 cells expressing Wnt4. The samples shown in *Q* and *R* were stained with an anti-E-cadherin antibody and DAPI. (Scale bars, 100 μm.) (*S–V*) Metanephric mesenchyme was cultured on L-cells expressing Wnt9. The samples shown in *U* and *V* were stained with an anti-E-cadherin antibody and DAPI. (Scale bars, 100 μm.)

DEVELOPMENTAL BIOLOGY

acting downstream of *Sall1*, because *Sall1*-null mice also show impaired ureteric bud attraction (7).

To examine whether the developmental potency of the mesenchyme after ureteric bud attraction was impaired in the absence of *Kif26b*, the mutant mesenchyme was separated from the ureteric buds and cultured on 3T3 feeder cells expressing Wnt4, a potent inducer of the mesenchyme-to-epithelial transition (13, 14). Almost all of the wild-type (11 of 11) (Fig. 2*O*) and mutant (6 of 7) (Fig. 2*P*) mesenchymes formed tubular structures within 3 days, and epithelial conversion was confirmed by E-cadherin staining (Fig. 2 *Q* and *R*). Because Wnt9b is an initial inducer secreted from the ureteric buds (3), we also confirmed the mesenchyme-to-epithelial transition in wild-type (5 of 5) and mutant (4 of 4) mesenchymes using feeder cells expressing Wnt9b (Fig. 2 *S*–*V*). Thus, the *Kif26b*-deficient mesenchyme retains its potency for epithelial conversion, but the failure of ureteric bud attraction probably causes subsequent defects in kidney development.

Kif26b Is Essential for the Maintenance of GDNF. GDNF is a major ureteric bud attractant. *Gdnf* was not properly maintained in the *Kif26b*-null mesenchyme at E11.5 (Fig. 3*A*), although its initial expression was intact until E10.75 (Fig. 3*B*). Phosphorylation of ERK and expression of *Wnt11*, which are both induced in ureteric tips by GDNF signaling (15), were also reduced (Fig. 3*A*). In contrast, Wnt9b was still expressed in the ureteric bud stalks (Fig. 3*A*). The *Gdnf* reduction was not caused by loss of mesenchymal cells, because we did not observe increased apoptosis evaluated by cleaved caspase-3 staining (Fig. S3*A*). Moreover, $Kif26b^{+/-}Gdnf^{+/-}$ mice showed more severe kidney phenotypes than $Kif26b^{+/-}$ or $Gdnf^{+/-}$ mice (Table 1), indicating there was a genetic link between *Kif26b* and the *Gdnf* pathway. Therefore, failure of *Gdnf* maintenance in the mutant embryos is likely to explain the phenotypic abnormalities in the ureteric bud attraction.

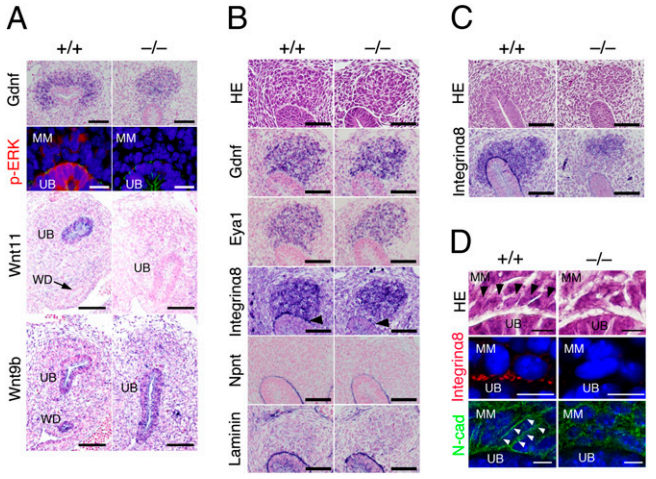

Fig. 3. Impaired condensation and *Gdnf* maintenance in the *Kif26b*-null mesenchyme. (*A*) Reduced expression of *Gdnf* and downstream signaling events in *Kif26b* mutant embryos at E11.5. Sections at E11.5 were stained by in situ hybridization for *Gdnf* and *Wnt11*, or immunostained for p-ERK (red) and pan-cytokeratin (green). Wnt9b is still expressed in the ureteric bud stalks. MM, metanephric mesenchyme; UB, ureteric bud; WD, Wolffian duct. (Black scale bars, 100 μm; white scale bars, 20 μm.) (*B* and *C*) Altered integrin α8 localization in the *Kif26b*-null metanephric mesenchyme. Sections at E10.75 (*B*) or E11.0 (*C*) were stained with hematoxylin and eosin, stained by in situ hybridization for *Gdnf* and *Eya1*, or immunostained for integrin α8, nephronectin (Npnt), and laminin. Integrin α8 is detected at the interface between the mesenchyme and the ureteric bud (arrowhead) in the wild-type embryos, but not in the mutant embryos. Integrin α8 is also reduced in the mutant mesenchyme adjacent to the ureteric buds. (Scale bars, 100 μm.) (*D*) Impaired condensation of the *Kif26b*-null mesenchyme at E10.75. Sections were stained with hematoxylin and eosin or immunostained for integrin α8 (red) or N-cadherin (green) for metanephric regions. Black arrowheads, columnar mesenchymal cells adjacent to ureteric buds; white arrowheads, lateral expression of N-cadherin in condensed mesenchymal cells. Nuclei were visualized by DAPI staining. (Scale bars, 10 μm.)

Kif26b Is Essential for the Adhesion and Polarization of Mesenchymal Cells Surrounding Ureteric Buds. *Gdnf* initiation is regulated by several transcription factors such as Pax2 and Eya1, while *Gdnf* is maintained by interactions between the mesenchyme and the ureteric buds including the integrin α8-mediated pathway (2). Indeed, Pax2 and *Eya1* were expressed in the mutant metanephric mesenchyme (Fig. 3*B* and Fig. S3*B*). In contrast, integrin α8 expression in mesenchymal cells adjacent to ureteric buds, as well as that clearly detected at the interface between the mesenchyme and the ureteric buds in wild-type embryos, was not observed in the mutant embryos at E10.75 when *Gdnf* was still expressed (Fig. 3*B*). Reduced integrin α8 expression in the mutant mesenchyme was more apparent at E11.0 (Fig. 3*C*). The integrin α8 ligand nephronectin and a basement protein laminin displayed no obvious differences between wild-type and mutant embryos (Fig. 3*B*). Double-staining for Sall1 and integrin α8 also confirmed that integrin α8 was reduced at the ureteric bud/mesenchyme junction when the mesenchyme was in contact with the ureteric bud (Fig. S3*C*). Therefore, integrin α8 reduction is unlikely to be secondary to the lack of ureteric bud invasion. The reduced ERK phosphorylation observed in the mutant mesenchyme (Fig. 3*A*) could imply impaired integrin signaling in this population. A reduction of integrin α8 in the mesenchyme close to the ureteric buds was also observed in *Kif26b* mutant embryos with milder phenotypes, in which the ureteric buds invaded into the mesenchyme to some extent (Fig. S3*D*). Thus, mutant mesenchymal cells that make contact with the ureteric bud tips were unable to establish the polarized localization of integrin α8, which probably led to the failure of *Gdnf* maintenance.

The mesenchymal cells adjacent to the ureteric buds were tightly cohered laterally and exhibited columnar alignment in the wild-type embryo, representing the initial histological indication of an interaction between the mesenchyme and the ureteric buds (Fig. 3*D*, black arrowheads). These mesenchymal cells showed a polarized distribution of integrin α8 on the basal side facing the ureteric buds (Fig. 3*D*). Basolateral N-cadherin staining also revealed that there was a strip of mesenchymal cells that exhibited columnar shapes along the ureteric bud tips in the wild-type embryo (Fig. 3*D*, white arrowheads). However, this condensation was not apparent in *Kif26b*-null mesenchymal cells adjacent to the ureteric bud tips (Fig. 3*D*). Therefore, mesenchymal cells that directly contact the ureteric buds could lose their basolateral integrity in the absence of *Kif26b*.

Similar abnormalities, including impaired integrin α8 and N-cadherin staining, were observed in the *Sall1*-deficient mesenchyme (Fig. S1*C*). Therefore, Kif26b could play a major functional role downstream of Sall1.

Table 1. Exacerbation of kidney phenotypes in compound mutant mice for *Kif26b* and *Gdnf*

Genotype	Kidney phenotypes			
	Normal	Hypoplasia	Agenesis	Total
$Kif^{+/-}$	50 (100)	0 (0)	0 (0)	50 (100)
$Gdnf^{+/-}$	39 (75.0)	4 (7.7)	9 (17.3)	52 (100)
$Kif^{+/-}Gdnf^{+/-}$	24 (46.2)	15 (28.8)*	13 (25.0)	52 (100)

The kidney phenotypes were analyzed at postnatal day 0. The data represent the number (percentage).
*$P < 0.01$, $Kif^{+/-}Gdnf^{+/-}$ mice vs. $Gdnf^{+/-}$ mice by the χ^2 test.

Kif26b Affects Cell Adhesion via an Interaction with Nonmuscle Myosin Heavy Chain II. To more closely study the role of Kif26b in the morphological changes of mesenchymal cells, we generated three independent human embryonic kidney (HEK) 293 cell lines overexpressing Flag-tagged Kif26b in a tetracycline-dependent manner. Each clone aggregated dramatically within 24 h in the presence of tetracycline (Fig. 4*A* and Fig. S4*A*). The cells showed enhanced calcium-dependent cell–cell adhesion, as assessed by dissociation assays (Fig. 4*B*). Indeed, knockdown of N-cadherin by a siRNA reduced the aggregation of Kif26b-overexpressing cells (Fig. 4*C* and Fig. S4 *C* and *D*). There were no significant changes in the expression levels of *Gdnf* and other transcription factors related to kidney development (Fig. S5*A*). The GDNF concentration was not increased in the supernatants (Fig. S5*B*). Thus, N-cadherin-dependent cell–cell adhesion is likely to be a primary event caused by Kif26b.

Many Kif proteins containing N-terminal motor domains interact with other molecules through their C-terminal regions (10). Indeed, cell aggregation was not observed when Kif26b lacking the C-terminal region (Kif26bΔC) was overexpressed in a tetracycline-dependent manner (Fig. 4*A*). The induction of the truncated proteins was more robust than that of the full-length protein, but the cells still exhibited no morphological changes (Fig. S4 *A* and *B*). Thus, we performed a pull-down assay using the GST-tagged C-terminal region of Kif26b, followed by mass spectrometry (Fig. 4*D*). Among the candidates, nonmuscle myosin heavy chain type IIB (NMHC IIB; MYH10) was confirmed as an interacting protein by coimmunoprecipitation experiments (Fig. 4*E*). Immunoprecipitation of MYH10 with deletion con-

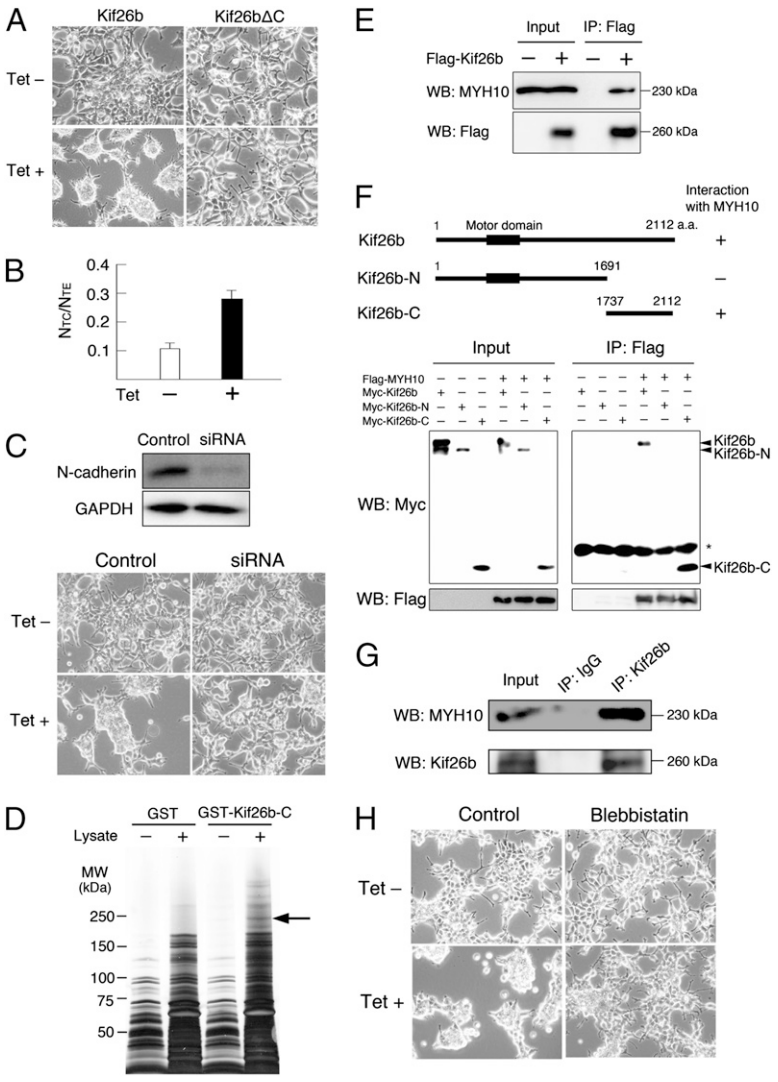

Fig. 4. Enhanced aggregation and cell adhesion by Kif26b overexpression. (*A*) Increased cell aggregation by Flag-tagged Kif26b overexpression. HEK293 cells were cultured for 48 h with or without tetracycline. No morphological changes are observed after overexpression of Kif26b lacking a C-terminal region (Kif26bΔC). (*B*) Increased calcium-dependent cell adhesion after Kif26b overexpression. Cells were incubated with (TC treatment) or without (TE treatment) calcium. Dissociation of the cells is represented by the index N_{TC}/N_{TE}, where N_{TC} and N_{TE} are the numbers of cell clusters after the TC and TE treatments, respectively. (*C*) Reduced aggregation by N-cadherin knockdown with a siRNA. Knockdown of N-cadherin was confirmed by immunoblotting. (*D*) GST pull-down complexes were analyzed by SDS/PAGE and silver staining. The arrow indicates the band for MYH10. (*E*) Interaction of Kif26b and MYH10. Immunoprecipitation was performed using HEK293 cells expressing tetracycline-inducible Flag-tagged Kif26b. (*F*) Deletion constructs of Kif26b and interaction of the C-terminal region of Kif26b and MYH10. Flag-MYH10 is coprecipitated with myc-tagged Kif26b. (*G*) Interaction of endogenous Kif26b and MYH10. MYH10 is coprecipitated with Kif26b from newborn mouse kidney lysates. (*H*) Effect of the NMHC II inhibitor blebbistatin on cell aggregation induced by tetracycline. Microscopic images of HEK293 cells incubated with and without tetracycline and blebbistatin for 24 h are shown.

structs of Kif26b also confirmed the specific interaction of the C-terminal region of Kif26b and MYH10 (Fig. 4*F*). The endogenous association of Kif26b and MYH10 was further confirmed using newborn kidney lysates (Fig. 4*G* and Fig. S6*A*). MYH10 was not only expressed in the mesenchyme but also in the ureteric buds, whereas Kif26b expression was specific to the mesenchyme (Fig. S6*B*), indicating an overlap of the expression domains of these two proteins. Furthermore, a specific NMHC II inhibitor, blebbistatin, inhibited the effect of Kif26b-dependent cell aggregation (Fig. 4*H*). These results suggest that Kif26b could regulate cell adhesion by interacting with NMHC II. Because accumulating evidence suggests that NMHC II augments cell adhesion by regulating actin filaments and cadherins (16), we propose that Kif26b may enhance the interaction of NMHC II and actin, thereby stabilizing the cell–cell adhesion of mesenchymal cells in the developing kidney.

Kif26b Is Not Required for the Function of Cilia. Finally, because another kinesin protein, Kif3, is involved in the transport of cilia components in the embryonic kidney, we examined the effect of Kif26b on cilia (17, 18). Impairment of cilia formation in renal tubules leads to polycystic kidney diseases (19). Cilia also play important roles in signaling pathways including Shh (20), which is required for kidney development (21). However, when we overexpressed Kif26b in MDCK cells that had well developed cilia on their surface, Kif26b was localized in the cytosol, and not in the cilia (Fig. S7*A*). Cilia were also detected in the metanephric mesenchyme in both wild-type and *Kif26b*-deficient mice (Fig. S7*B*). Furthermore, when we genetically reduced the *Kif26b* alleles from heterozygous mice for *Shh* or its downstream effecter *Gli3*, the mice displayed no renal phenotypes (Fig. S7*C*). Therefore, *Kif26b* is unlikely to be involved in either cilia formation or Shh signaling.

Discussion

We have shown that *Kif26b*, a kinesin family gene, is essential for embryonic kidney development. Kif26b plays an important role in the compact adhesion between mesenchymal cells adjacent to the ureteric buds, possibly by interacting with nonmuscle myosin. This could lead to the establishment of the basolateral integrity of the mesenchyme and the polarized expression of integrin α8, which maintains the Gdnf expression required for further ureteric bud attraction.

Recently, it was reported that another kinesin-11 member, Kif26a, negatively regulates Gdnf-Ret signaling by binding to Grb2 in Ret-expressing enteric neurons (22). However, Kif26a is not expressed in the developing kidney. In addition, Kif26b is expressed in the Gdnf-expressing kidney mesenchyme, but not in Ret-expressing ureteric buds, and eventually exerts positive effects on Gdnf expression. Therefore, the molecular mechanism of Kif26b is distinct from that of Kif26a.

NMHC II plays an important role in cell adhesion because it provides tension for actin filaments, and this is required for the proper localization of cell adhesion proteins such as cadherins (16). *MYH9*-deficient embryonic stem cells and mouse embryos exhibit a loss of cell–cell adhesion (23), while *MYH10*-null mice show hydrocephalus caused by loss of cell–cell adhesion in the cells lining the spinal canal (24). In addition, Smy1p, a kinesin-11 member in *Saccharomyces cerevisiae*, induces a conformational change in the class V myosin Myo2p, which enhances its interaction with actin and causes cell protrusion in one direction (25, 26). Moreover, NMHC II-actin complexes appear to facilitate cross-talk between N-cadherin and integrins during cardiac development (27, 28). Therefore, we speculate that Kif26b may enhance the interaction of NMHC II and actin, thereby stabilizing the cell–cell adhesion of mesenchymal cells and the interaction between the mesenchyme and ureteric buds through integrins in the developing kidney.

It is known that Kif3 regulates N-cadherin expression on the cell surface by associating with KAP3, and that *KAP3*-deficient embryonic fibroblasts show impaired N-cadherin expression (29). However, Kif26b was not detected in fibroblasts. Therefore, Kif26b is unlikely to ubiquitously regulate N-cadherin transport.

To the best of our knowledge, this is the first report that a kinesin deficiency can cause the lack of an entire organ. Better understanding of the kinesin-mediated regulation in the kidney primordia will provide unique insights into organ development.

Experimental Procedures

Cloning of *Kif26b*. A 5.5-kb cDNA was obtained from the Mammalian Gene Collection (National Institute of Health) but lacked a 5′ portion as judged by a sequence comparison with the human *KIF26B* cDNA. We found another cDNA in the mouse database that showed homology to the 5′ portion of the human *KIF26B* cDNA and the 5′ region of the mouse *Kif26b* genome. RT-PCR using mouse embryos (E13.5) showed that the combined cDNA existed in vivo. The amplified fragments were sequenced and a comparison between the resultant cDNA and the mouse genome revealed an exon/intron structure of *Kif26b* that was compatible with that of human *KIF26B*.

Generation of *Kif26b*-Deficient Mice. A *Kif26b*-targeting vector was constructed by incorporating the 5′ 7.8-kb *Kif26b* genomic and 3′ 4.4-kb *Kif26b* fragments. Both fragments were amplified by PCR using LA Taq (Takara) into a vector that contained the β-galactosidase gene (*lacZ*), the neomycin resistance (*Neo*^{r}) gene (*PGK-Neo*), and the diphtheria toxin A subunit (pMC1DTA) in tandem (30) (details of the vector are available from www.cdb.riken.go.jp/arg/cassette.html). The targeting vector was electroporated into TT2 ES cells, and 3 of 192 G418-resistant clones were correctly targeted, as determined by PCR and Southern blotting analyses using 5′ or 3′ probes after XmnI or AseI digestion, respectively. Two ES clones were used to generate germline chimeras that were bred with C57BL/6J female mice. Mice homozygous for the *Kif26b*-targeted allele (accession no. CDB0440K; www.cdb.riken.jp/arg/mutant%20mice%20list.html) were obtained by intercrossing heterozygous mice. Even when *Neo*^{r} was deleted by crossing the *Kif26b* mutant mice with mice expressing Flp, the phenotypes and lacZ expression patterns were identical to those of the original mutant mice. Genotyping of the offspring was performed by PCR using a forward primer, 5′-CCATCACATGCAGAAGGCTA-3′, and two reverse primers, 5′-AGCATCGAAGGCAAACATCT-3′ and 5′-CCGTAATGGGATAGGTCACG-3′, producing products of 300 bp for the wild-type allele and 500 bp for the mutant allele. Northern blotting was performed using 4 mg of poly(A)+ RNA from E11.5 embryos per lane. Either a 5′ SalI-BamHI 1.25-kb fragment or a 3′ SphI-NheI 1.5-kb fragment was used as a probe.

In Situ Hybridization and Immunohistochemistry. Samples were fixed in 10% formalin and processed for paraffin-embedded sectioning. In situ hybridization and immunostaining were performed using an automated Discovery System (Ventana) according to the manufacturer's protocols (31). A 5′ 1.2-kb SalI-BamHI fragment or a 3′ 639-bp PCR-amplified fragment of the *Kif26b* cDNA was subcloned, and transcripts were generated with T7 RNA polymerase and DIG-RNA labeling mix (Roche). Both probes showed similar expression patterns. Other probes were isolated by PCR or were described previously (32).

For fluorescence immunohistochemistry, paraffin-embedded sections were deparaffinized and autoclaved at 121 °C for 5 min in citrate buffer (pH 6.0). After incubation in blocking solution for 1 h at room temperature, the sections were incubated overnight with primary antibodies at 4 °C, followed by incubation with secondary antibodies conjugated with Alexa Fluor 488 or 594 (Invitrogen). For whole-mount staining, metanephric explants were fixed with 4% paraformaldehyde, blocked with 1% BSA, and incubated overnight with primary antibodies at 4 °C, followed by incubation with secondary antibodies. The primary antibodies used were: anti-Sall1 (31) (Perseus Proteomics); anti-cleaved caspase-3 (Cell Signaling); anti-pan-cytokeratin (Sigma); anti-E-cadherin (BD Transduction Laboratories); anti-phosphorylated Erk (Cell Signaling); anti-α8 integrin (1); anti-N-cadherin (Santa Cruz Biotechnology); anti-MYH10 (Cell Signaling or Developmental Studies Hybridoma Bank); and anti-acetylated α-tubulin (Sigma). A polyclonal antibody against mouse nephronectin was produced by immunizing rabbits with FLAG-tagged recombinant mouse nephronectin (33). The antibody was purified by affinity chromatography using columns of 6× His-tagged mouse nephronectin immobilized on CNBr-activated Sepharose 4B (GE Healthcare). We generated a polyclonal anti-Kif26b antibody by immunizing rabbits with GST-fused Kif26 protein (amino acids 1402–2112). The specificity of the anti-Kif26b antibody was confirmed using *Kfi26b*-null kidney sections.

GST Pull-Down Assay and Mass Spectrometry. The C-terminal *Kif26b* fragment corresponding to amino acids 1737–2112 was cloned into *pGEX6P-1* (GE Healthcare) and introduced into BL21 (DE3). GST-fused Kif26b protein bound to Glutathione-Sepharose 4B beads (GE Healthcare) was incubated with newborn kidney or brain samples lysed in buffer [50 mM Tris·HCl (pH 7.5), 0.5 M NaCl, 5 mM EDTA, 1% Triton X-100, 1 mM PMSF, protease inhibitor mixture]. The beads were then washed and boiled in SDS/PAGE sample buffer. The eluents were analyzed by Silver Quest (Invitrogen) and candidate bands were subjected to mass spectrometry.

Organ Culture of the Metanephric Mesenchyme. Organ culture experiments were performed as described in refs. 7 and 8. Briefly, metanephroi were dissected from E11.5 embryos and the ureteric buds were removed after 5 min of incubation with 0.2% collagenase (Sigma). The mesenchyme rudiments were cultured on 3T3Wnt4 cells or L-Wnt9b cells at the air-fluid interface on a polycarbonate filter (0.4 μm; Corning) supplied with DMEM plus 10% FCS (3, 13, 14).

Generation of Cell Lines Expressing Tetracycline-Inducible Kif26b. The SalI-NotI fragment of Flag-tagged *Kif26b* was cloned into the EcoRV-NotI site of a pcDNA5/FRT/TO vector and transfected into Flp-In T-Rex HEK293 cells (Invitrogen). Stable transformants were selected following the manufacturer's instructions. All of the isolated clones showed identical induction of Kif26b in the presence of tetracycline (1 μg/mL). For inducible induction of *Kif26bΔC*, a 3.0-kb SalI-MluI fragment was cloned into the EcoRV site of the pcDNA5/FRT/TO vector. For dissociation assays, the cells were treated with 0.01% trypsin in Hepes-buffered calcium- and magnesium-free Puck's saline (HCMF) supplemented with 1 mM $CaCl_2$ (TC treatment) or 1 mM EDTA (pH 7.5) (TE treatment) for 15 min at 37 °C, respectively, followed by pipetting 10 times. The extent of the cell dissociation was represented by the index N_{TC}/N_{TE}, where N_{TC} and N_{TE} were the numbers of cell clusters after the TC and TE treatments, respectively (34). For NMHC II inhibition, 100 μg/mL (–)-blebbistatin (Calbiochem) and its negative control (+)-blebbistatin (Calbiochem) were used.

ACKNOWLEDGMENTS. We thank K. Shinmyozu and A. Nakamura for mass spectrometry; A. Nagafuchi, K. Oozono, J. Usui, M. Takeichi, M. A. Conti, and R. S. Adelstein for technical advice; M. Takasato and T. Ohmori for technical assistance; and L. F. Reichardt, N. D. Rosenblum, and A. P. McMahon for providing the anti-integrin α8 antibody, a protocol for cilia staining, and Wnt-expressing feeder cells, respectively. The monoclonal antibody against MYH10 developed by G. W. Conrad was obtained from the Developmental Studies Hybridoma Bank developed under the auspices of the National Institute of Child Health and Human Development (NICHD) and maintained by the University of Iowa. This work was supported in part by Grants-in-Aid from the Ministry of Education, Culture, Sports, Science, and Technology (MEXT) and the Global COE Program (Cell Fate Regulation Research and Education Unit, MEXT, Japan).

1. Müller U, et al. (1997) Integrin α8β1 is critically important for epithelial-mesenchymal interactions during kidney morphogenesis. *Cell* 88:603–613.
2. Linton JM, Martin GR, Reichardt LF (2007) The ECM protein nephronectin promotes kidney development via integrin α8β1-mediated stimulation of Gdnf expression. *Development* 134:2501–2509.
3. Carroll TJ, et al. (2005) Wnt9b plays a central role in the regulation of mesenchymal to epithelial transitions underlying organogenesis of the mammalian urogenital system. *Dev Cell* 9:283–292.
4. Nishinakamura R (2008) Stem cells in the embryonic kidney. *Kidney Int* 73:913–917.
5. Self M, et al. (2006) Six2 is required for suppression of nephrogenesis and progenitor renewal in the developing kidney. *EMBO J* 25:5214–5228.
6. Kobayashi A, et al. (2008) Six2 defines and regulates a multipotent self-renewing nephron progenitor population throughout mammalian kidney development. *Cell Stem Cell* 3:169–181.
7. Nishinakamura R, et al. (2001) Murine homolog of SALL1 is essential for ureteric bud invasion in kidney development. *Development* 128:3105–3115.
8. Osafune K, Takasato M, Kispert A, Asashima M, Nishinakamura R (2006) Identification of multipotent progenitors in the embryonic mouse kidney by a novel colony-forming assay. *Development* 133:151–161.
9. Takasato M, et al. (2004) Identification of kidney mesenchymal genes by a combination of microarray analysis and Sall1-GFP knockin mice. *Mech Dev* 121:547–557.
10. Miki H, Okada Y, Hirokawa N (2005) Analysis of the kinesin superfamily: Insights into structure and function. *Trends Cell Biol* 15:467–476.
11. Hirokawa N, Noda Y (2008) Intracellular transport and kinesin superfamily proteins, KIFs: Structure, function, and dynamics. *Physiol Rev* 88:1089–1118.
12. Yamashita K, Sato A, Asashima M, Wang PC, Nishinakamura R (2007) Mouse homolog of SALL1, a causative gene for Townes-Brocks syndrome, binds to A/T-rich sequences in pericentric heterochromatin via its C-terminal zinc finger domains. *Genes Cells* 12: 171–182.
13. Stark K, Vainio S, Vassileva G, McMahon AP (1994) Epithelial transformation of metanephric mesenchyme in the developing kidney regulated by Wnt-4. *Nature* 372: 679–683.
14. Kispert A, Vainio S, McMahon AP (1998) Wnt-4 is a mesenchymal signal for epithelial transformation of metanephric mesenchyme in the developing kidney. *Development* 125:4225–4234.
15. Majumdar A, Vainio S, Kispert A, McMahon J, McMahon AP (2003) Wnt11 and Ret/Gdnf pathways cooperate in regulating ureteric branching during metanephric kidney development. *Development* 130:3175–3185.
16. Conti MA, Adelstein RS (2008) Nonmuscle myosin II moves in new directions. *J Cell Sci* 121:11–18.
17. Nonaka S, et al. (1998) Randomization of left-right asymmetry due to loss of nodal cilia generating leftward flow of extraembryonic fluid in mice lacking KIF3B motor protein. *Cell* 95:829–837.
18. Corbit KC, et al. (2008) Kif3a constrains beta-catenin-dependent Wnt signalling through dual ciliary and non-ciliary mechanisms. *Nat Cell Biol* 10:70–76.
19. Lin F, et al. (2003) Kidney-specific inactivation of the KIF3A subunit of kinesin-II inhibits renal ciliogenesis and produces polycystic kidney disease. *Proc Natl Acad Sci USA* 100:5286–5291.
20. Singla V, Reiter JF (2006) The primary cilium as the cell's antenna: Signaling at a sensory organelle. *Science* 313:629–633.
21. Yu J, Carroll TJ, McMahon AP (2002) Sonic hedgehog regulates proliferation and differentiation of mesenchymal cells in the mouse metanephric kidney. *Development* 129:5301–5312.
22. Zhou R, Niwa S, Homma N, Takei Y, Hirokawa N (2009) KIF26A is an unconventional kinesin and regulates GDNF-Ret signaling in enteric neuronal development. *Cell* 139: 802–813.
23. Conti MA, Even-Ram S, Liu C, Yamada KM, Adelstein RS (2004) Defects in cell adhesion and the visceral endoderm following ablation of nonmuscle myosin heavy chain II-A in mice. *J Biol Chem* 279:41263–41266.
24. Ma X, Bao J, Adelstein RS (2007) Loss of cell adhesion causes hydrocephalus in nonmuscle myosin II-B-ablated and mutated mice. *Mol Biol Cell* 18:2305–2312.
25. Lillie SH, Brown SS (1994) Immunofluorescence localization of the unconventional myosin, Myo2p, and the putative kinesin-related protein, Smy1p, to the same regions of polarized growth in Saccharomyces cerevisiae. *J Cell Biol* 125:825–842.
26. Beningo KA, Lillie SH, Brown SS (2000) The yeast kinesin-related protein Smy1p exerts its effects on the class V myosin Myo2p via a physical interaction. *Mol Biol Cell* 11: 691–702.
27. Linask KK, Manisastry S, Han M (2005) Cross talk between cell-cell and cell-matrix adhesion signaling pathways during heart organogenesis: Implications for cardiac birth defects. *Microsc Microanal* 11:200–208.
28. Lu W, et al. (2008) Cellular nonmuscle myosins NMHC-IIA and NMHC-IIB and vertebrate heart looping. *Dev Dyn* 237:3577–3590.
29. Teng J, et al. (2005) The KIF3 motor transports N-cadherin and organizes the developing neuroepithelium. *Nat Cell Biol* 7:474–482.
30. Murata T, et al. (2004) ang is a novel gene expressed in early neuroectoderm, but its null mutant exhibits no obvious phenotype. *Gene Expr Patterns* 5:171–178.
31. Sakaki-Yumoto M, et al. (2006) The murine homolog of SALL4, a causative gene in Okihiro syndrome, is essential for embryonic stem cell proliferation, and cooperates with Sall1 in anorectal, heart, brain and kidney development. *Development* 133:3005–3013.
32. Kobayashi H, Kawakami K, Asashima M, Nishinakamura R (2007) Six1 and Six4 are essential for Gdnf expression in the metanephric mesenchyme and ureteric bud formation, while Six1 deficiency alone causes mesonephric-tubule defects. *Mech Dev* 124:290–303.
33. Sato Y, et al. (2009) Molecular basis of the recognition of nephronectin by integrin alpha8beta1. *J Biol Chem* 284:14524–14536.
34. Nagafuchi A, Ishihara S, Tsukita S (1994) The roles of catenins in the cadherin-mediated cell adhesion: Functional analysis of E-cadherin-alpha catenin fusion molecules. *J Cell Biol* 127:235–245.